Dalton Transactions

Cite this: *Dalton Trans.*, 2012, **41**, 11330

www.rsc.org/dalton

PAPER

Combining aspects of the platinum anticancer drugs picoplatin and BBR3464 to synthesize a new family of sterically hindered dinuclear complexes; their synthesis, binding kinetics and cytotoxicity†

Sarah D. Brown,[a] Katherine D. Trotter,[a] Oliver B. Sutcliffe,[b] Jane A. Plumb,[c] Bruce Waddell,[a] Naomi E. B. Briggs[a] and Nial J. Wheate*[d]

Received 12th June 2012, Accepted 12th July 2012
DOI: 10.1039/c2dt31313h

Picoplatin is a sterically hindered mononuclear platinum drug undergoing clinical trials. The 2-methylpyridine ring provides steric hindrance to the drug, preventing attack from biological nucleophiles. BBR3464 is a trinuclear platinum drug which was recently in Phase II clinical trials, and is highly cytotoxic both *in vitro* and *in vivo*; it derives this activity through the flexible adducts it forms with DNA. In this work we sought to combine the properties of both drugs to synthesise a family of sterically hindered, dinuclear platinum complexes as potential anticancer agents. The bis-pyridyl-based ligands were synthesised through a peptide coupling reaction using diaminoalkanes of differing lengths (n = 2, 4 or 8) and 4-carboxypyridine or 2-methyl-4-carboxypyridine. The resultant dinuclear platinum complexes were synthesised by reacting two equivalents of transplatin or mono-aquated transplatin to each ligand, followed by purification by precipitation with acetone. The unprotected complexes react faster with 5′-guanosine monophosphate (drug to nucleotide ratio 1 : 2; $t_{1/2}$ = 2 h), glutathione (1 : 10, $t_{1/2}$ = 55 min) and human serum albumin (HSA) (1 : 1, $t_{1/2}$ = 24 h) compared to their hindered, protected equivalents (5′-guanosine monophosphate, $t_{1/2}$ = 3.5 h; glutathione = 1.7 h; HSA, $t_{1/2}$ = 110 h). The complexes were tested for *in vitro* cytotoxicity in the A2780 and A2780/cp70 ovarian cancer cell line. The unprotected platinum complexes were more cytotoxic than their protected derivatives, but none of the complexes were able to overcome resistance. The results provide important proof-of-concept for the development of a larger family of sterically hindered multinuclear-based platinum complexes.

Introduction

The use of small molecule drugs for the treatment of human and animal cancers remains an important component of treating the disease and is no better demonstrated than by the drug cisplatin (Fig. 1), the parent compound of the platinum-based family of anticancer drugs.[1,2] The metal complex binds to its target, DNA, *via* coordination bonds and distorts the normal three-dimensional structure of the double helix.[3,4] This subsequently induces cell death through apoptosis.[5,6] The success of cisplatin is limited, however, by its poor selectivity for cancerous cells, which causes severe toxic side effects[7] and the ability of some tumours to develop resistance to drug treatment.[1,8,9]

Since the approval of cisplatin in 1979, thousands of analogues have been examined in an effort to produce less toxic derivatives, drugs that can be administered orally, or drugs that are able to circumvent tumour resistance.[2,10,11] Whilst 23 platinum-based drugs have undergone clinical trials, only two

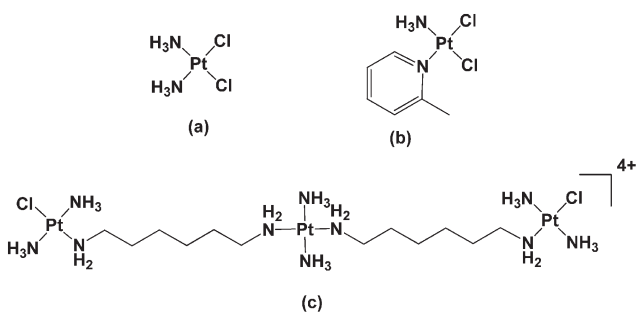

Fig. 1 The chemical structures of (a) cisplatin, (b) picoplatin and (c) BBR3464. Counter ions for BBR3464 are usually either 4(Cl^-) or 4(NO_3^-).

[a]*Strathclyde Institute of Pharmacy and Biomedical Sciences, University of Strathclyde, 161 Cathedral Street, Glasgow, G4 0RE, UK*
[b]*Division of Chemistry and Environmental Science, School of Science and the Environment, Manchester Metropolitan University, Chester Street, Manchester, M1 5GD, UK*
[c]*Institute of Cancer Sciences, College of Medical, Veterinary and Life Sciences, University of Glasgow, Cancer Research UK Beatson Laboratories, Garscube Estate, Glasgow, G61 1BD, UK*
[d]*Faculty of Pharmacy, The University of Sydney, NSW 2006, Australia. E-mail: nial.wheate@sydney.edu.au*

†CCDC 870360. For crystallographic data in CIF or other electronic format see DOI: 10.1039/c2dt31313h

(carboplatin and oxaliplatin) have gained worldwide marketing approval.[1,2] One drug currently in Phase II and III clinical trials is *cis*-amminedichlorido(2-methylpyridine)platinum(II), also known as ZD0473 or picoplatin (see Fig. 1).[1,12,13] This drug was designed specifically to overcome glutathione-mediated drug resistance. Picoplatin's reactivity towards soft nucleophiles is attributed to its stereochemistry;[12] the 2-methylpyridine (picoline) ring sits almost perpendicular to the plane of the platinum ligands, which places the methyl group above the platinum atom.[14] The location of the methyl in this position provides direct steric protection of the platinum atom, effectively slowing both drug aquation and binding by cysteine/methionine residues in peptides and proteins.[14–16]

Another drug of particular interest is BBR3464, a trinuclear complex (see Fig. 1), which displayed excellent activity in cisplatin sensitive and resistant cancers in both *in vitro* and *in vivo* models.[10,17,18] Whilst cisplatin forms short range, rigid, intrastrand cross-links, BBR3464 forms flexible, long and short range, inter- and intrastrand cross-links upon binding,[19] as well as inducing B- to Z- and B- to A-type DNA conformational changes.[18,20] Preclinical trials revealed cytotoxicity at concentrations one thousand times lower than the concentration required by cisplatin;[18] however, in human Phase I trials, systemic toxicity was found to be so severe that the maximum tolerated dose was just 0.9–1.1 mg m^{-2}, compared to cisplatin with an administrable dose of 20–120 mg m^{-2}.[1] In Phase II trials, BBR3464 was also found to be ineffective in all tumours examined.[18,21,22] Model studies suggest that this might be due to a combination of the low doses that can be administered and the high reactivity and rapid degradation of the drug *in vivo*.[23,24]

We have therefore hypothesised that a new family of platinum-based drugs could be developed that incorporate the steric protection of picoplatin with the flexible long range DNA adduct formation of BBR3464 (Scheme 1). Such drugs may be highly cytotoxic but, because they are less susceptible to degradation and protein binding, may also have less severe systemic side-effects with more drug reaching tumours intact. In this paper, we describe the synthesis of our first proof-of-concept compounds starting with a family of dinuclear platinum complexes with pyridine- and 2-methylpyridine-based bridging linkers of different lengths. These complexes were characterised by ^{1}H NMR, ^{195}Pt NMR, electrospray ionisation mass spectrometry (ESI-MS) and elemental analysis. Their reaction kinetics using 5′-guanosine monophosphate, glutathione and human serum albumin were examined to see the effectiveness of the bridging ligand in providing steric protection to the complexes. Finally, the dinuclear complexes were tested for *in vitro* cytotoxicity *via* growth inhibition assays using the human ovarian cancer cell line A2780 and its cisplatin resistant sub-line A2780/cp70.

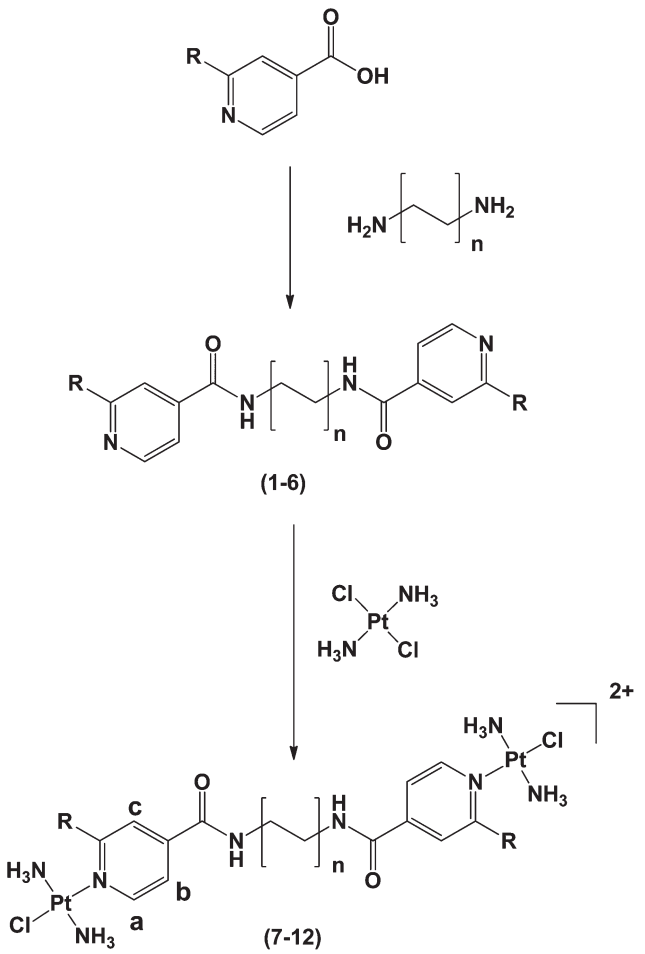

Scheme 1 The synthetic method of the bispyridyl ligands and their subsequent dinuclear platinum complexes, showing the hydrogen labelling scheme used for the aromatic protons **1**, $n = 2$, R = H; **2**, $n = 4$, R = H; **3**, $n = 8$, R = H; **4**, $n = 2$, R = CH_3; **5**, $n = 4$, R = CH_3; **6**, $n = 8$, R = CH_3; **7**, $n = 2$, R = H; **8**, $n = 4$, R = H; **9**, $n = 8$, R = H; **10**, $n = 2$, R = CH_3; **11**, $n = 4$, R = CH_3; **12**, $n = 8$, R = CH_3.

Results and discussion

Ligand synthesis

No suitable ligand was commercially available for use as the bridging ligand of the sterically hindered platinum complexes. Such a ligand requires two pyridyl groups linked by a flexible chain. It was preferable that the chain of the ligand come in various lengths so that its effect on cytotoxicity could be evaluated. Flexibility is also important so that the pyridyl groups have free rotation thus allowing them to position themselves with the 2-methyl groups over the platinum atom. In addition, it was preferable to have two versions of the ligand; one with a 2-methyl group, and one without, so that the amount of steric protection could be fully evaluated. We therefore chose ligands **1–6** and synthesised them from the peptide coupling of 4-carboxypyridine or 2-methyl-4-carboxypyridine to diaminoalkanes of variable length ($n = 2$, 4 or 8; Scheme 1). The synthesis of the unmethylated ligands has previously been reported,[25] but their 2-methyl derivatives have not. The benefit of these ligands is their ease of synthesis, as peptide coupling reactions are routine to conduct and have high yields. More importantly, synthesis *via* peptide coupling produces ligands with two amide groups. For multinuclear platinum complexes it has been shown that hydrogen bonding and electrostatic binding between the bridging ligand and the DNA helix is important in stabilising and directing the type of DNA adducts formed.[19,26–28] The ligands synthesised in this work are therefore capable of acting as both hydrogen bond acceptors/donors and when pre-associated in the

DNA minor groove, can potentially form hydrogen bonds to the bases as well as ion–dipole interactions with the anionic DNA backbone.

All four ligands were characterised by ^{1}H and ^{13}C NMR, ESI-MS and their purity (>99%) confirmed by elemental analysis. The free unmethylated bispyridyl ligands (**1–3**) display two doublets in the ^{1}H NMR aromatic region and either two or four resonances in the aliphatic region depending on the diaminoalkane used. For the methylated bispyridyl ligands (**4–6**) the loss of symmetry due to the 2-methyl group gives rise to two doublet resonances (Scheme 1; H_a and H_b) and one singlet resonance (H_c), as well as the expected aliphatic resonances, including a large resonance for the methyl group at 1.29 or 1.56 ppm. For both the unmethylated and methylated free ligands, formation of the peptide bond is observed by the large shift of the amine resonance from a broad peak around 3–4 ppm for the free diaminoalkane to a broad triplet upon coupling between 8.65 to 8.80 ppm for the amide proton.

Ligand pseudo-polymorphism

The commercial development of any drug is not made solely on the basis of its activity *in vitro* and *in vivo*, but will also include elements of: the potential market and revenue, its ease/cost of synthesis, its stability during manufacture and storage, its solubility, drug polymorphism or pseudo-polymorphism, and the drug's ability to be made into appropriate dosage forms. Whilst making the ligands used for the synthesis of the platinum complexes it was found that all could be recrytallised from hot water and formed either plate-like sheets or rectangular crystals and the type of crystalline ligands formed was dependent on the rate of crystallisation. Elemental analysis of the different crystalline materials found that, where there was a difference, this was due to the formation of hydrates. Powder X-ray diffraction was used to show that these hydrates are pseudo-polymorphs which can convert to the anhydrous form upon heating or standing for short periods of time (for example see Fig. 2). As this could affect their production during manufacture, we sought to examine this in more detail.

Ligand **3** was analysed by differential scanning calorimetry (DSC) and thermogravimetric analysis (Fig. 3). As can be seen, the sample shows water loss in the first heat cycle, with onset mass loss (TGA curve) occurring at the same temperature (92 °C) as the first endothermic transition in the DSC curve. The DSC curve stabilises before the next endothermic transition which corresponds to a melting temperature of 131 °C. On the following heat cycle an exothermic transition begins at 44 °C which corresponds to the crystallisation temperature. In this cycle, the TGA curve remains stable and no mass loss occurs, with the only endothermic transition this time observed for the sample melting, again at 131 °C. This result therefore shows that the initial formation of hydrates is unlikely to be a problem during manufacture if batches are properly dried before use in the synthesis of the platinum complexes, as the ligands themselves are not hygroscopic once dried.

In some cases different crystal types were formed by a few ligands that did not correspond to hydrates. To examine if this is due to polymorphism, the powder form of ligand **2** was analysed by powder X-ray diffraction and the XRPD pattern used to determine if there were differences to the structure determined by single crystal X-ray diffraction. Pawley-type fit to the data (data not shown), in which background, zero-point, peak shape and unit cell parameters describing the profile were refined, yielded a unit cell of dimensions (a, b, c = 26.7143, 5.6299, 10.0695 Å; α, β, γ (°) = 90.0, 101.496, 90.0). Comparison with the single crystal data[25] (a, b, c = 26.519, 5.637, 10.084 Å; α, β, γ (°) = 90, 101.36, 90) confirms that the polycrystalline sample is consistent with the single crystal X-ray structure. Background subtracted XRPD data returns a χ^2 of 1.207, and a flat difference plot indicates that the sample was pure phase.

For one ligand, **5**, single crystals suitable for X-ray analysis were grown allowing its solid-state structure to be accurately determined. The asymmetric unit of the sterically hindered linker contains two crystallographically independent molecules and two waters of hydration. One linker molecule is well ordered (Fig. 4 and Table 1) whereas the butyldicarboxamide linker in the second is disordered over two locations. A feature of the solid-state packing is the 180° rotation about the carbonyl–pyridyl sigma bond in the disordered moiety, causing the methyl groups to orientate in the opposite direction. In comparison to the unmethylated linker, which features a doubly penetrated network, the methylated linker behaves differently due to the loss of inherent symmetry whereby it forms discrete alternating layers linked by a hydrogen bonding network *via* solvated water molecules in the channels. This structural change arises due to the pyridyl proton involved in the hydrogen bonding network being replaced by a methyl group and is therefore no longer able to participate in the same fashion.

Metal complex synthesis

Formation of the dinuclear platinum complexes **7–12** was achieved through the reaction of either transplatin, or monoaquated transplatin, with the ligands **1–6** in hot water for 6–12 h. The coordination of the platinum to the methylated ligands is considerably more difficult, presumably due to the steric protection of the pyridyl-nitrogen atom by the methyl group. As such, the platination reactions were usually conducted for longer time periods with mono-aquated transplatin and even then resulted in lower yields compared to the unprotected complexes. The platinum complexes were purified by dissolving them in a minimum amount of hot water, cooling and then fractionally precipitating with acetone. Acetone is added slowly until the solution just turns opaque; this first precipitate is the impurity. Addition of more acetone (10–20 mL) makes the solution very cloudy and filtration through a nylon filter (0.2 or 0.45 μm) removes what appears to be impurity leaving the platinum complexes in solution; which are then recovered by freeze drying or rotary evaporation. Sometimes the acetone precipitation purification step needs to be repeated 2–3 times, especially for the protected complexes, to get the metal complexes to better than 99% purity by elemental analysis and ^{1}H NMR.

It is important to note that both the purification of the free ligands and the dinuclear platinum complexes is based on their precipitation from the solvent (in most cases water). The yield and the ease by which this is done is highly dependent on both the concentration of the product and the quantity being

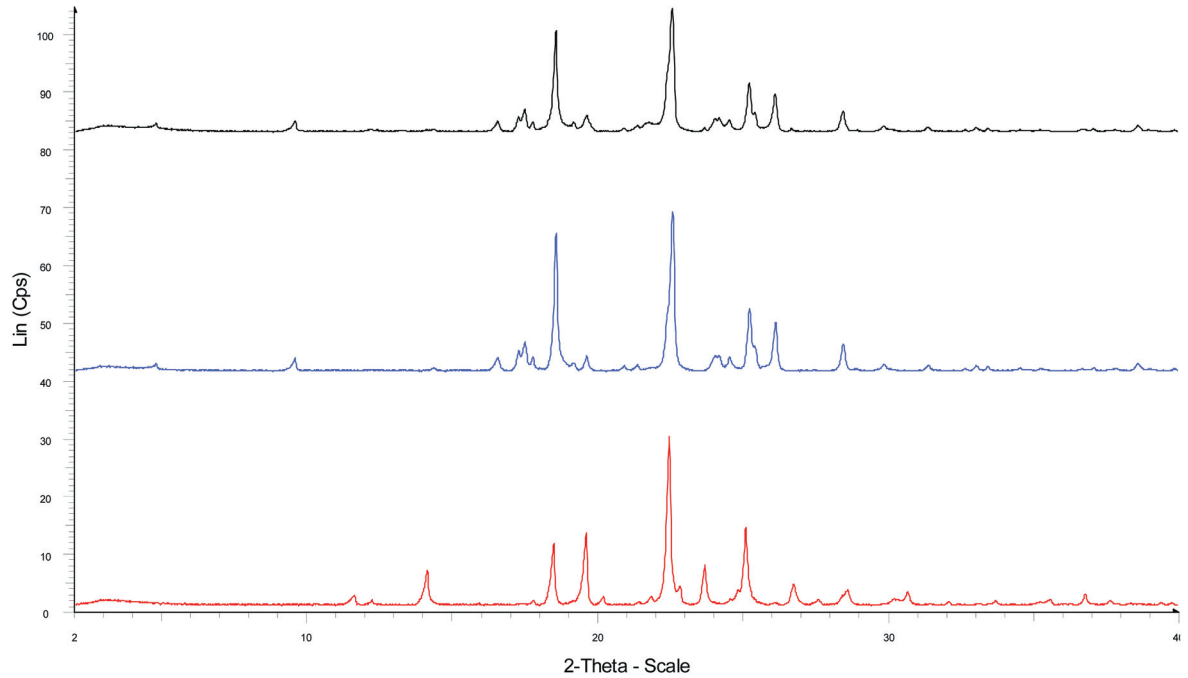

Fig. 2 The X-ray powder diffraction pattern of **2** showing (bottom) the hydrated form of the ligand produced from its rapid crystallisation from water, (middle) the anhydrous crystalline form of the ligand produced from its slow crystallisation from water and (top) the same sample from the bottom spectrum upon standing for 2 days showing its conversion to the anhydrous state.

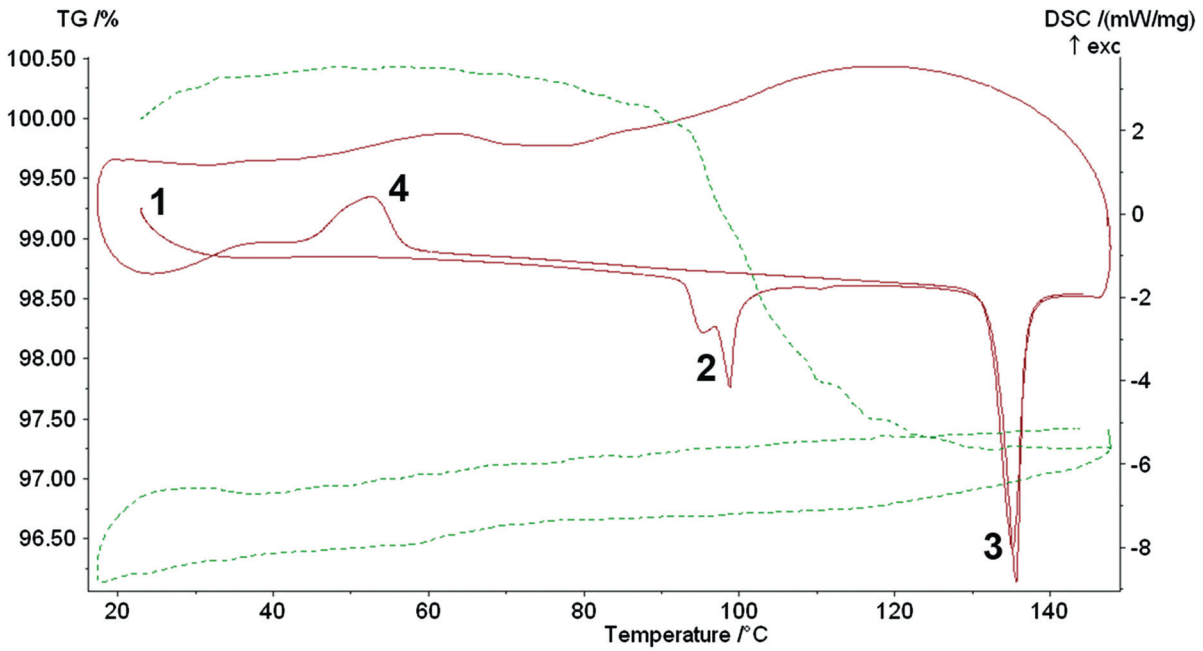

Fig. 3 Simultaneous and thermogravimetric analysis (green) and differential scanning calorimetry (red line) showing change in input energy (milliwatts per milligram) as a function of temperature, giving (1) the start of the DSC trace, (2) water loss from the crystal, (3) ligand melting and (4) sample recrystallisation, for ligand **3**.

synthesised/purified. The larger the quantity/higher the concentration the easier and more successful the synthesis becomes. At low concentrations/quantities (*e.g.* <50 mg) both the free ligands and the platinum complexes can be difficult to precipitate and obtain as pure compounds.

The dinuclear platinum complexes were characterised by ^{1}H, ^{195}Pt NMR, ESI-MS and their purity (>98%) confirmed by elemental analysis. Coordination of platinum to all four ligands is observed by the downfield shifts of the aromatic resonances of the bispyridyl ligands in the ^{1}H NMR spectra. For the

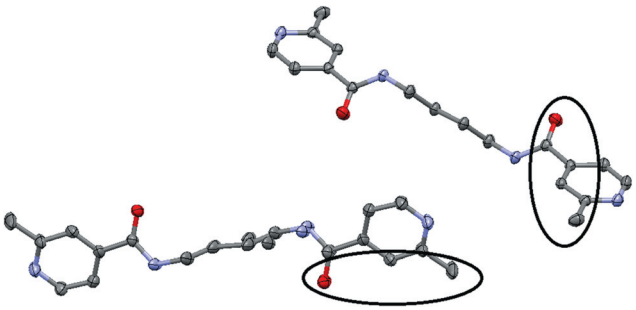

Fig. 4 The single crystal X-ray structure of the methylated bis-pyridyl ligand **5**, showing the *cis*- and *trans*-orientations of the carbonyl groups to the 2-methyl groups in the two independent molecules of the unit cell, with the slight disorder of two of the methylene carbon atoms demonstrated on the bottom structure.

Table 1 Single crystal X-ray diffraction data for the methylated ligand **5**

Crystal data	Values
Empirical formula	$C_{36}H_{52}N_8O_8$
Formula weight	725.00
Temperature	123(2) K
Wavelength	0.71073 Å
Crystal system, space group	Triclinic, *P*1
Unit cell dimensions	a = 7.3486(3) Å, α = 66.270(5)°
	b = 12.1524(7) Å, β = 77.808(4)°
	c = 12.3530(6) Å, γ = 72.732(4)°
Volume	959.05(8) Å^3
Z, Density (calculated)	1, 1.255 Mg m^{-3}
Absorption coefficient	0.090 mm^{-1}
F (000)	388
Crystal size	0.2 × 0.2 × 0.1 mm
Theta range for data collection	2.92° to 27.00°
Limiting indices	$-9 \le h \le 9$, $-15 \le k \le 15$, $-15 \le l \le 15$
Reflections collected/unique	12 777/4185 [R(int) = 0.0160]
Completeness to theta = 27.00	99.9%
Absorption correction	Semi-empirical from equivalents
Max and min transmission	1.00000 and 0.81603
Refinement method	Full-matrix least-squares on F^2
Data/restraints/parameters	4185/79/273
Goodness-of-fit on F^2	1.029
Final R indices [$I > 2\sigma(I)$]	R_1 = 0.0450, wR_2 = 0.1090
R indices (all data)	R_1 = 0.0521, wR_2 = 0.1153
Largest diff. peak and hole	0.301 and −0.443 e Å^3

unprotected complexes the H_a resonance (see Scheme 1 for proton labelling details) moves downfield by 0.25 ppm and the H_b by 0.03 ppm. For the protected complexes, the H_a, H_b and H_c resonances shift 0.5, 0.04 and 0.2 ppm, respectively. Broad platinum coupling is also seen at the base of the H_a resonance for all six dinuclear platinum complexes and a broad peak representing the $-NH_3$ groups is sometimes observed around 4 ppm in freshly prepared samples, before it disappears from solvent exchange.

The ^{195}Pt NMR spectra also clearly indicate coordination of the platinum to all six ligands. Both the unprotected and protected platinum complexes show a single resonance in the region of ~−2300 ppm which is in the region observed for similar platinum complexes that contain two *trans*-ammine ligands and an aromatic amine *trans* to a chlorido ligand.[29,30] No resonances in the region of −2100 or −1800 ppm are observed, which indicates there is no free transplatin, or free aquated-transplatin remaining.[30]

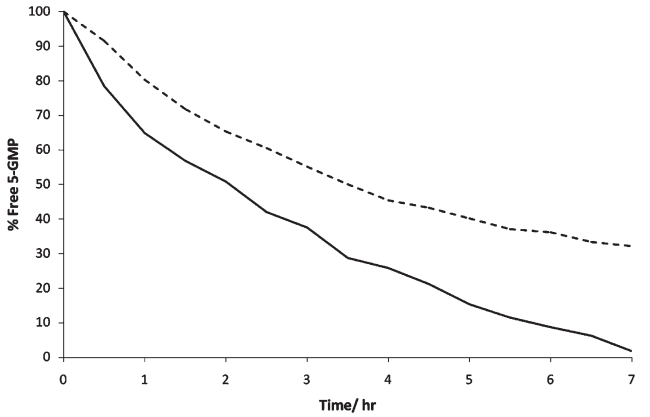

Fig. 5 A plot of the percentage free of 5′-guanosine monophosphate as a function of time during its reaction with the unprotected dinuclear platinum complex **8**, solid line, and the sterically protected derivative **11**, dashed line.

Platinum complex binding kinetics

In designing our sterically hindered multinuclear platinum complexes we sought to combine the steric protection of the 2-methyl pyridine ligand of picoplatin with the flexible DNA adduct formation of multinuclear platinum drugs. Whilst the incorporation of steric bulk is mainly to prevent degradation by thiol peptides, *i.e.* glutathione,[31] our sterically hindered complexes should display slower reaction rates with all biological nucleophiles, including DNA.[15,16] As such, we conducted three different kinetic experiments to examine the effect of the 2-methyl group on the reaction rates of the platinum complexes.

5′-Guanosine monophosphate. As a first experiment, and for simplicity, we chose 5′-guanosine monophosphate (5′-GMP) as a model for DNA binding using ^{1}H NMR. Upon coordination of platinum at the N7 of guanosine, the nucleotide's H8 resonance shifts from ~8.1 to ~8.7 ppm. Both resonances are clearly resolvable in ^{1}H NMR spectra and so the amount of each species can be determined by simply integrating the relative size of each resonance. The unprotected dinuclear platinum complex **8** which contains the butane-based linker (n = 4) and its protected derivative **11** were incubated with two equivalents of 5′-guanosine monophosphate at 37 °C for time periods up to 7 h. The ^{1}H NMR spectra, which were then used to generate a plot of the percent of free guanosine as a function of time (Fig. 5), demonstrate that the protected platinum complex **11** reacts nearly two-fold slower compared with the unprotected complex **8**. Whilst the sterically protected complex **11** has a reaction half-life of ~3.5 h, the unprotected complex **8** has a half-life of just ~2 h and has fully reacted with the guanosine by 7 h.

Glutathione. Next, the rate of reaction of **8** and **11** with glutathione was analysed by ^{1}H NMR spectroscopy. Glutathione was incubated with the metal complexes in a 10 : 1 ratio to mimic the

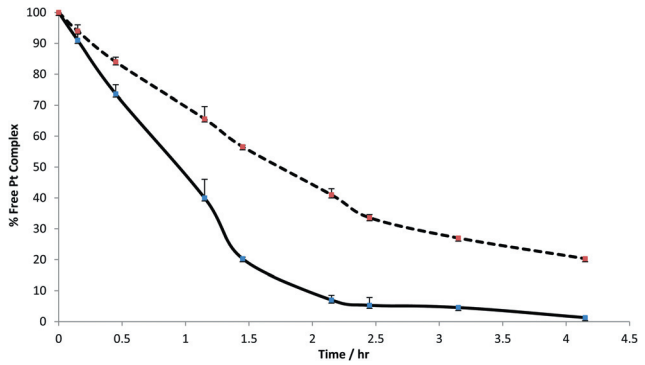

Fig. 6 A plot of the percentage amount of unbound platinum complex as a function of time with glutathione at 37 °C, showing the faster rate of reaction of the unprotected dinuclear platinum complex **8**, solid line, compared with its equivalent sterically hindered, protected complex **11**, dashed line.

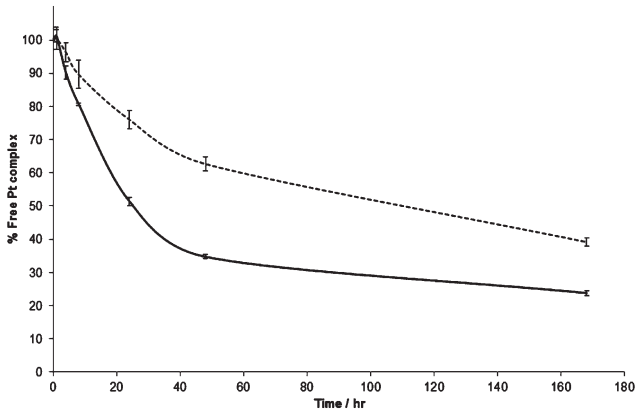

Fig. 7 A plot of the percentage amount of unbound platinum complex as a function of time with human serum albumin at 37 °C, showing the faster rate of reaction of the unprotected dinuclear platinum complex **8**, solid line, compared with its equivalent sterically hindered, protected complex **11**, dashed line.

high concentrations of the peptide inside the cell. As glutathione has no aromatic resonances, the degradation of the metal complexes can easily be followed through the appearance of additional resonances in the aromatic ^{1}H NMR region. The metal complexes have either two or three resonances for the free drug, but as the complexes react with glutathione additional resonances are observed between 8 and 9 ppm. As the reaction proceeds these peaks increase, then decrease, in size until only resonances representing uncoordinated bridging ligands are observed. Relative integration of the resonances allowed us to plot the percentage of free metal complex as a function of time and determine the reaction half-lives of complexes **8** and **11** (Fig. 6). As expected, the unprotected complex **8** reacted quickest with a half-life of 55 min. The sterically protected complex **11** in contrast reacts almost two-fold slower with a half-life of 1.7 h.

Human serum albumin. As well as binding to intracellular nucleophiles, a large amount of administered platinum drug is bound by proteins in blood serum. Human serum albumin (HSA) is the most abundant protein in human blood serum and has been shown to readily bind to platinum drugs.[32–36] It was therefore of interest to examine the reaction kinetics of the protected and unprotected dinuclear platinum drugs with HSA and see if any protection against HSA binding was afforded to the protected complex.

The unprotected dinuclear platinum complex **8** and its protected derivative **11** were incubated with a stoichiometric equivalent of HSA (mole of metal complex to mole of protein) in phosphate-buffered saline (pH 7.4) at 37 °C for time periods up to 168 h. At intervals, aliquots were taken from the reaction mixture and immediately centrifuged on Viva-spin columns. All HSA and HSA-bound platinum remained in the top of the column, with all unbound platinum complex washed to the bottom. The quantity of unbound platinum was then determined using UV-visible spectrophotometry (248/249 nm) which then allowed the percentage free platinum in solution to be determined at each time point. A plot of free complex as a function of time demonstrates that the unprotected and protected complexes display similar kinetics to those seen in the 5′-GMP and glutathione experiments as the sterically hindered complex **11** reacted significantly more slowly with HSA than the unprotected complex **8**. The unprotected platinum complex **8** has a HSA reaction half-life of 24 h, whereas the protected complex **11** reacts more than 4.5-fold slower, with a half-life of approximately 110 h (Fig. 7).

Table 2 The *in vitro* cytotoxicity of the protected and unprotected dinuclear platinum complexes in the human ovarian carcinoma cell line A2780 and its cisplatin-resistant derivative A2780/cp70, given as the IC_{50}; the concentration of metal complex required to inhibit cell growth by 50%

Complex	Methyl-protection	Linker length	IC_{50} (μM) A2780	IC_{50} (μM) A2780/cp70
Cisplatin	N/A	N/A	0.24	2.55
BBR3464[47]	N/A	N/A	0.01 ± 0.007	n.d.[a]
Picoplatin[47]	N/A	N/A	1.15 ± 0.4	n.d.[a]
7	No	2	0.90 ± 0.15	12.5 ± 1.8
10	Yes	2	1.75 ± 0.11	31.3 ± 4.5
8	No	4	0.028 ± 0.002	2.19 ± 0.3
11	Yes	4	0.14 ± 0.01	14.3 ± 0.06
9	No	8	0.054 ± 0.008	1.38 ± 0.2
12	Yes	8	1.54 ± 0.2	9.85 ± 0.5

[a] n.d. = not determined.

In vitro cytotoxicity

The cytotoxicity of the six dinuclear platinum complexes was determined using *in vitro* growth inhibition assays with the human ovarian carcinoma cell line A2780 and its cisplatin resistant sub-line A2780/cp70 (Table 2). The results suggest two clear trends: first that there is an ideal linker length. The most active dinuclear complexes (**8** and **11**) contain the $n = 4$ linker followed by the complexes made by the $n = 8$ linker (**9** and **12**). The complexes made using the shortest linker (**7** and **10**; $n = 2$) were least active. This is consistent with structure–activity

studies of other multinuclear platinum complexes from the BBR3464 family which has found that the ideal methylene chain length is six carbon units.[18] Linkers shorter or longer than this length were found to produce metal complexes that were less cytotoxic. Both our $n = 4$ and $n = 8$ ligands are longer than this ideal length, although the shorter length of the $n = 4$ ligand means it is closer to the preferred end-to-end distance, and hence, results in more cytotoxic metal complexes.

Secondly, the protected complexes are less active than the unprotected derivatives. This result is not unexpected given the short incubation periods used in *in vitro* assays and the reduced rate of reaction that the protected complexes will have in comparison to the unprotected derivatives; their slower reaction rates mean the onset of apoptosis is later and hence the cells reproduce more before the effects of the complexes are felt. This reduced cytotoxicity is also observed for picoplatin when compared with cisplatin, and has been demonstrated in a panel of 11 different cell lines, where picoplatin displayed IC_{50} values that were 3.1-fold higher than those for cisplatin.[12] This is due to picoplatin's slower aquation and rate of reaction; about 2-fold slower than cisplatin and similar to the slower rate of reaction observed for the protected complexes in this work. This reduced cytotoxicity of picoplatin was not a concern as the reduced reactivity also led to much reduced toxicity.[37] This gives picoplatin a higher therapeutic index compared with cisplatin; an effect we are trying to mimic with these sterically hindered dinuclear complexes. Unfortunately, none of the six platinum complexes are able to overcome resistance, although this result is not necessarily surprising. The dinuclear derivative of BBR3464, called BBR3005, is also not able to overcome resistance in many different matched cell lines including A2780 pairs.[38–40]

Conclusions

In this work we have prepared a family of six dinuclear platinum anticancer complexes based on the chemical structures of the sterically hindered platinum drug picoplatin and the conformationally flexible multinuclear platinum drugs, of which BBR3464 is the lead agent. Two versions of each ligand were made; with and without methylation at the 2-position of the pyridine ring to examine the effect of steric hindrance on the subsequent platinum complexes. The protected dinuclear platinum complex **11**, reacts significantly more slowly with 5′-guanosine monophosphate, glutathione and human serum albumin compared with the equivalent unprotected dinuclear platinum complex **8**. The reduced rate of reaction with HSA by the protected platinum complex may be both a function of slower reaction kinetics, and also, different pre-association effects with the protein.

The reduced rates of reaction of the protected complexes are similar in magnitude to that observed for picoplatin compared with cisplatin. *In vitro* cytotoxicity assays demonstrate that there is an ideal linker length (around four methylene groups in the bridging linker), and the protected complexes are less active than the unprotected complexes. The latter result is consistent with their slow reaction with nuclear DNA and is similar to the reduced *in vitro* cytotoxicity of picoplatin compared with cisplatin. Overall these results provide important proof-of-concept data for the development of drugs that are able to overcome drug resistance, but are also resistant to deactivation and degradation. In particular, we hypothesise that with suitable modification of the bis-pyridine linkers, such that only one side of the ligand is protected, we can synthesize the trinuclear platinum-based complexes. Such trinuclear complexes would better mimic the structure of BBR3464 while still having steric protection to the terminal platinum groups. We hope to make a family of these trinuclear complexes in the future.

Experimental

Materials

All reagents were purchased from Sigma Aldrich with the exception of 1-propylphosphonic acid cyclic anhydride (T3P) and anhydrous dimethylformamide which were purchased from Alfa Aesar. Viva-spin columns with a molecular mass cut off of 5000 daltons were purchased from VWR.

Instrument methods

Elemental analyses were performed on a Perkin Elmer 240 Elemental Analyser. ^{1}H and ^{13}C NMR were recorded on a JEOL 400 MHz spectrometer, whereas ^{195}Pt and kinetics studies were recorded on a Bruker DPX 400 MHz spectrometer. ^{195}Pt NMR resonances were referenced externally to a sample of K_2PtCl_4 in D_2O at −1631 ppm.[41] Positive ion ESI-MS were recorded on a Finnigan LTQ Orbitrap. Samples were dissolved in H_2O to a concentration of 100 μM and injected into the instrument in 90% CH_3CN/10% H_2O at a flow rate of 400 μL min^{-1}. The capillary temperature and voltage were 200 °C and 40 V, respectively, with a source voltage of 4000 V. UV-vis experiments were conducted on a Varian Cary 50 Bio spectrophotometer at a wavelength of 249 nm for (**8**; ε = 13 665 M^{-1} cm^{-1}) and 248 nm for (**11**; ε = 16 182 M^{-1} cm^{-1}).

Synthesis of pyridyl-based linkers

Diaminoalkane (1.13 mmol) and 4-carboxypyridine (4.19 mmol, 3 eq.) were dissolved in anhydrous dimethylformamide (2 mL). To this, triethylamine (945 μL, 6.8 eq.) was added and the reaction stirred at room temperature, for 3 h, under a nitrogen atmosphere. The flask was then cooled to 0 °C and 1-propylphosphonic acid cyclic anhydride (1.5 mL, 2.35 eq.) was added slowly with stirring. The flask was allowed to warm to room temperature and stirred for 2 days. The reaction mixture was diluted with water and extracted against diethyl ether (3 × 100 mL) and the aqueous layer was separated (at this point the linker made using 1,4-diaminobutane precipitates from solution). Sodium hydrogen carbonate solution (1% w/v, 100 mL) was added to the aqueous layer and stirred overnight at room temperature to yield a fine, yellow precipitate which was collected by filtration, washed with diethyl ether and air dried.

***N,N′*-(Ethane-1,2-diyl)diisonicotinamide (1).** Yield: 87%. Elemental analysis: $C_{14}H_{14}N_4O_2$ requires: C, 62.21; H, 5.22; N, 20.73%. Found: C, 61.88; H, 5.41; N, 20.74%. ^{1}H NMR (400 MHz, d_6-DMSO, ppm) 8.91 (2H, t), 8.72 (4H, d), 7.73

(4H, d), 3.47 (4H, m). ^{13}C NMR (100 MHz, d_6-DMSO, ppm) 165.5, 150.8, 142.0, 121.8, 39.9. ESI-MS $[M - H]^+$ found: 271.1 *m*/*z*, requires 271.1.

***N*,*N*′-(Butane-1,4-diyl)diisonicotinamide (2).** Yield: 79%. Elemental analysis: $C_{16}H_{18}N_4O_2$ requires: C, 64.41; H, 6.08; N, 18.78%. Found: C, 64.27; H, 6.02; N, 18.65%. ^{1}H NMR (400 MHz, d_6-DMSO, ppm): 8.77 (2H, t), 8.71 (4H, d), 7.73 (4H, d), 1.58 (4H, m). ^{13}C NMR (100 MHz, d_6-DMSO, ppm) 165.1, 150.8, 142.1, 121.8, 26.6 (2C). ESI-MS $[M + H]^+$ found: 299.13 *m*/*z*, requires: 299.15; $[M + Na]^+$ found: 321.07 *m*/*z*, requires: 321.13.

***N*,*N*′-(Octane-1,8-diyl)diisonicotinamide (3).** Yield: 91%. Elemental analysis: $C_{20}H_{26}N_4O_2$ requires: C, 67.77; H, 7.39; N, 15.81%; Found: C, 67.29; H, 7.42; N, 15.56%. ^{1}H NMR (400 MHz, d_6-DMSO, ppm) 8.73 (2H, t), 8.70 (4H, d), 7.74 (4H, d), 3.25 (4H, q), 1.52 (4H, t), 1.30 (8H, s). ^{13}C NMR (100 MHz, d_6-DMSO, ppm) 165.1, 150.7, 142.1, 121.7, 29.4, 29.3, 26.9 (2C). ESI-MS: $[M + H]^+$ requires: 355.21 *m*/*z*, found 355.24.

Synthesis of 2-methylpyridyl-based linkers

Diaminoalkane (1 mmol) and 2-methyl-4-carboxypyridine (411 mg, 3 eq.) were dissolved in anhydrous dimethylformamide (4 mL). To this, triethylamine (833 μL, 6 eq.) was added and the reaction stirred at room temperature, for 3 h, under a positive pressure of nitrogen. The flask was then cooled to 0 °C and 1-propylphosphonic acid cyclic anhydride added (1.4 mL, 2.2 eq.) The flask was allowed to warm to room temperature and stirred for 2 days.

***N*,*N*′-(Ethane-1,2-diyl)bis(2-methylisonicotinamide) (4).** The reaction mixture was diluted with water and NaOH added. Upon cooling a white precipitate formed, which was collected by vacuum filtration, washed with water and air dried. Slow evaporation of a saturated aqueous solution yielded crystalline material. Yield: 96%. Elemental analysis: $C_{16}H_{18}N_4O_2{\cdot}3H_2O$ requires: C, 54.53; H, 6.86; N, 15.90%. Found: C, 54.33; H, 6.66; N, 15.76%. ^{1}H NMR (400 MHz, d_6-DMSO, ppm) 8.85 (2H, t), 8.56 (2H, d), 7.61 (1H, s), 7.53 (2H, d), 3.45 (4H, m) 2.52 (6H, s). ^{13}C NMR (100 MHz, d_6-DMSO, ppm) 165.8, 159.2, 150.0, 142.4, 121.2, 118.9, 39.6, 24.63. ESI-MS $[M + H]^+$ requires: 299.35 *m*/*z*, found: 299.1.

***N*,*N*′-(Butane-1,4-diyl)bis(2-methylisonicotinamide) (5).** The reaction mixture was diluted with water and extracted against diethyl ether (3 × 150 mL). The aqueous layer was separated and 20% NaOH solution (w/v, 50 mL) was added. The solution was allowed to sit at room temperature for 3 days until a precipitate appeared. This was then filtered and dried to yield a fine, yellow powder. Slow evaporation of a saturated aqueous solution yielded single crystals suitable for X-ray diffraction. Yield: 89%. Elemental analysis: $C_{18}H_{22}N_4O_2{\cdot}2.5H_2O$ requires: C, 58.21, H, 7.33 N, 15.08%. Found: C, 58.17; H, 7.26; N, 14.99%. ^{1}H NMR (400 MHz, d_6-DMSO, ppm) 8.73 (2H, t), 8.55 (2H, d), 7.61 (2H, s), 7.53 (2H, d), 3.29 (4H, d), 1.56 (6H, s). ^{13}C NMR (100 MHz, d_6-DMSO, ppm) 165.3, 159.2, 150.0, 142.5, 121.1, 118.9, 27.0, 24.6 ppm. ESI-MS $[M + H]^+$ requires: 327.40 *m*/*z*, found: 327.18.

***N*,*N*′-(Octane-1,8-diyl)bis(2-methylisonicotinamide) (6).** On addition of water (100 mL), the product precipitated out of solution. This was then collected by filtration, washed with diethyl ether and allowed to air dry to produce a fine, silky powder. Yield: 91%. Elemental Analysis: $C_{22}H_{30}N_4O_2$ requires: C, 69.08; H, 7.91; N, 14.65%. Found: C, 69.00; H, 7.88; N, 14.31%. ^{1}H NMR (400 MHz, d_6-DMSO, ppm): 8.67 (2H, t), 8.55 (2H, d), 7.60 (2H, s), 7.52 (2H, d), 3.24 (4H, q), 1.51 (4H, t), 1.29 (6H, s). ^{13}C NMR (100 MHz, d_6-DMSO, ppm) 165.3, 159.2, 150.0, 142.5, 121.1, 118.9, 29.4, 29.2, 27.0, 24.6. ESI-MS $[M + H]^+$ requires: 383.47 *m*/*z*, found: 383.25.

Synthesis of unprotected platinum complexes

Ligand **1–3** (100 mg) and transplatin (2.1 eq.) were dissolved in water and heated to 55–60 °C with stirring for 5–6 h during which the solution turned colourless. Next, the solution was stirred at room temperature for 1–2 days in the dark. Water was then removed *in vacuo*. The remaining solid was dissolved in the minimum amount of hot water and acetone was added until the solution became cloudy. The precipitate was removed by filtration, the filtrate collected and the solvent removed by rotary evaporation. The process was repeated until the product, a pale yellow powder, was pure by ^{1}H NMR.

[Bis-{*trans*-diammineplatinum(II)}{μ-*N*,*N*′-(ethane-1,2-diyl)bis-(isonicotinamide)}] chloride hydrate, complex (7). Yield: 59%. Elemental analysis: $C_{14}H_{26}Cl_4N_8O_2Pt_2{\cdot}H_2O$ requires: C, 18.93; H, 3.18; N, 12.61%. Found: C, 19.18; H, 3.28; N, 12.36%. ^{1}H NMR (400 MHz, D_2O, ppm) 8.97 (4H, d), 7.76 (4H, d), 3.65 (4H, s). ^{195}Pt NMR (85 MHz, D_2O) −2299 ppm. ESI-MS: $[M + H]^+$ requires: 800.49 *m*/*z*, found 801.13.

[Bis-{*trans*-diammineplatinum(II)}{μ-*N*,*N*′-(butane-1,4-diyl)bis-(isonicotinamide)}] chloride, complex (8). Yield: 65%. Elemental analysis: $C_{16}H_{30}Cl_4N_8O_2Pt_2$ requires: C, 21.39; H, 3.37; N, 12.47%. Found C, 21.11; H, 3.21; N, 12.72%. ^{1}H NMR (400 MHz, D_2O, ppm) 8.95 (4H, d), 7.76 (4H, d), 3.41 (4H, s), 1.66 (4H, s). ^{195}Pt NMR (85 MHz, D_2O) −2299 ppm. ESI-MS: $[M]^{2+}$ requires: 413.07 *m*/*z*, found: 413.53; $[M]^+$ requires: 826.12 *m*/*z*, found: 826.00.

[Bis-{*trans*-diammineplatinum(II)}{μ-*N*,*N*′-(octane-1,8-diyl)bis-(isonicotinamide)}] chloride trihydrate, complex (9). Yield: 63%. Elemental analysis: $C_{20}H_{38}Cl_4N_8O_2Pt_2{\cdot}3H_2O$ requires: C, 23.82; H, 4.40; N, 11.11%. Found C, 23.95, H, 4.14, N, 11.20%. ^{1}H NMR (400 MHz, D_2O, ppm) 8.95 (4H, d), 7.76 (4H, d), 3.35 (4H, t), 1.56 (4H, t), 1.30 (8H, s). ^{195}Pt NMR (85 MHz, D_2O) −2299 ppm. ESI-MS *m*/*z* $[M]^+$ requires: 882.18 *m*/*z*, found: 882.00; $[M]^{2+}$ requires: 441.09 *m*/*z*, found: 441.80.

Synthesis of protected platinum complexes

Ligands **4–6** (50 mg) and mono-aquated transplatin (2.1 eq.) were dissolved in hot water (100 mL) and stirred in darkened conditions at 55–60 °C for 3 h. To the reaction mixture, THF was added (30–50 mL) and was allowed to stir with heating for

a further 3 h, then at room temperature for a further 2 days. Solvent was removed *in vacuo*. The remaining solid was dissolved in the minimum amount of hot water and acetone was added until the solution became cloudy. The solid was removed by filtration, the filtrate collected and the solvent removed by rotary evaporation. The process was repeated until the product was pure, giving a pale fluffy powder or glass-like solid.

[Bis-{*trans*-diammineplatinum(II)}{μ-*N*,*N*′-(ethane-1,2-diyl)bis-(2-methylisonicotinamide)}] chloride dihydrate, complex (10). Yield: 30%. Elemental analysis: $C_{16}H_{30}Cl_4N_8O_2Pt_2{\cdot}2H_2O$ requires: C, 18.53; H, 3.44; N, 12.35%. Found: C, 18.01; H, 3.29; N, 12.46%. ^{1}H NMR (400 MHz, D_2O, ppm): 8.94 (2H, d), 7.69 (2H, s) 7.51 (2H, d), 3.63 (4H, s), 3.12 (6H, s). ^{195}Pt NMR (85 MHz, D_2O) −2300 ppm. ESI-MS $[M]^{2+}$ requires: 826.12 *m*/*z*, found: 826.05.

[Bis-{*trans*-diammineplatinum(II)}{μ-*N*,*N*′-(butane-1,4-diyl)bis-(2-methylisonicotinamide)}] chloride dihydrate, complex (11). Yield: 49%. Elemental analysis: $C_{18}H_{34}Cl_4N_8O_2Pt_2{\cdot}2H_2O$ requires: C, 22.46, H, 3.98, N, 11.64%. Found: C, 22.17, H, 3.95, N, 11.83%. ^{1}H NMR (400 MHz, D_2O, ppm) 9.07 (4H, d), 7.80 (2H, s, CH), 7.57 (4H, d), 3.42 (2H, t), 3.13 (6H, s), 1.68 (4H, d). ^{195}Pt NMR (85 MHz, D_2O) −2316 ppm. ESI-MS $[M + Na]^+$ requires: 877.14 *m*/*z*, found: 878.00.

[Bis-{*trans*-diammineplatinum(II)}{μ-*N*,*N*′-(octane-1,8-diyl)bis-(2-methylisonicotinamide)}] chloride tetrahydrate, complex (12). Yield: 55%. Elemental analysis: $C_{22}H_{42}Cl_4N_8O_2Pt_2{\cdot}4H_2O$ requires: C, 25.05; H, 4.78; N, 10.62%. Found C, 25.18; H, 4.71; N, 10.43%. ^{1}H NMR (400 MHz, D_2O, ppm) 9.07 (4H, d), 7.57 (4H, d), 3.36 (4H, t), 3.13 (6H, s), 1.59 (4H, t), 1.34 (8H, s). ^{195}Pt NMR (85 MHz, D_2O) −2320 ppm. ESI-MS $[M + H]^+$ requires 911.00 *m*/*z*, found 912.00.

Differential scanning calorimetry/thermogravimetric analysis

Thermal behaviour, mass loss and melting point were monitored using simultaneous thermal analysis (STA), comprising DSC (differential scanning calorimetry) and TGA (thermal gravimetric analysis) analyses. This was carried out on a Netzsch STA 449 C thermocouple, equipped with a Netzsch CC 200 liquid nitrogen supply system and a Netzsch CC 200 C control unit. Analysis was performed using the Netzsch Proteus data analysis package. About 3 mg of sample was placed in a sealed crucible. This was then heated from 20–145 °C at 10 °C min^{-1}, cooled to 20 °C at 20 °C min^{-1} and again heated to 145 °C at 10 °C min^{-1}.

Single crystal X-ray diffraction

Crystals were coated in mineral oil and mounted on glass fibres. Data were collected at 123 K on a Bruker Nonius Apex II CCD diffractometer using monochromated Mo Kα radiation. The heavy atom positions were determined by Patterson methods and the remaining atoms located in difference electron density maps. Full-matrix least-squares refinement was based on F^2, with all non-hydrogen atoms anisotropic. While hydrogen atoms were mostly observed in the difference maps, they were placed in calculated positions riding on the parent atoms and were refined isotropically. The structure solution and refinement used the programs SHELX-86,[42] SHELX-97[42] and the graphical interface WinGX.[43] Absorption corrections were made with SADABS[44] and figures generated using Mercury 2.4. Selected crystallographic parameters are in Table 1 and full data and esd's are provided in the ESI.†

Powder X-ray diffraction

A sample was lightly ground in an agate mortar and pestle and filled into a 0.7 mm borosilicate glass capillary. The sample was mounted and aligned on a Bruker-AXS D8 Advance diffractometer and data were collected at room temperature in the range 4–35° 2θ (2 kW; Cu Kα_1, λ = 1.54056 Å; step size 0.015° 2θ step time = 1 s). The data from the polycrystalline sample were compared to the known single-crystal structure[25] using the software Dash 3.2 *via* a Pawley refinement[45] as implemented in TOPAS Academic v4.1.

Guanosine binding kinetics

Stock solutions of complexes **8** and **11** were prepared in D_2O, as was a solution of 5′-guanosine monophosphate. Complex **8** and **11** (1 mM) was added to an NMR tube followed by guanosine monophosphate (2 eq.) giving a total volume of 600 μL. Upon addition of guanosine monophosphate solution, a 1D water suppression proton scan was run at 37 °C and repeated every 30 min for 7.5 h.

Human serum albumin binding kinetics

Solutions containing stoichiometric equivalents of platinum complexes (**8** and **11**; 2 μmol) and HSA (2 μmol) were stirred and incubated at 37 °C in a phosphate buffer solution (pH 7.4) containing 100 mM NaCl for a maximum of 7 days (total sample volume 4.166 mL). Samples were taken periodically (250–350 μL; 0, 1, 2, 4, 8, 24, 48, 72, 168 h) and transferred to 2 mL Viva-spin columns with a 5000 dalton molecular mass cut-off filter. These were centrifuged at 8000 rpm for 25 min before the supernatant fluid containing the unbound platinum complex (200–250 μL) was collected and diluted to 750 μL with phosphate-buffered saline for analysis.

Glutathione binding kinetics

Solutions containing platinum complex (**8** and **11**) in D_2O were added to a solution of glutathione in D_2O to make a total volume of 600 μL with a platinum complex concentration of 2 mM and a glutathione concentration of 20 mM. The NMR tube was placed in the NMR spectrometer at 37 °C and kinetics runs were completed using 32 scans and a delay between each scan set of 30 min. The total amount of free and bound metal complex was determined by relative integration of the free platinum complex peaks compared to the new peaks which arise between 8 and 9 ppm.

In vitro growth assays

In vitro growth assays using the human ovarian cancer cell line A2780 were conducted using published methods.[46] Cells were grown in RPMI media containing 10% foetal calf serum, penicillin, streptomycin and L-glutamate in a 5% CO_2 atmosphere. The cells were trypsinised, counted and adjusted to 500–1000 cells per well. Cisplatin or metal complex stock solutions were diluted with RPMI to prepare a dilution series based on the total platinum concentration (0.1–100 μM). 10 μL aliquots were taken from these solutions and added in triplicate to each well along with RPMI only. The plates were further incubated for 24 h before the medium and drug was removed and replaced by fresh medium and incubated for a further 48 h. Plates were then fed with fresh medium and MTT solution (50 μL), wrapped in tinfoil and incubated for 4 h. The medium and MTT were removed from the wells leaving the purple MTT-formazan crystals. These were dissolved by addition of DMSO (200 μL) and glycine buffer (25 μL) to each well. Plates were then read by their absorbance at 570 nm with the resulting dose–response curve displaying absorbance (*y*-axis) with respect to drug concentration in μM (*x*-axis).

Abbreviations

5′-GMP	5′-guanosine monophosphate
DSC	differential scanning calorimetry
HSA	human serum albumin
TGA	thermogravimetric analysis
XRPD	X-ray powder diffraction

Acknowledgements

This worked was funded in part by a University of Strathclyde, Research Development Fund Grant, No. RDF1539. We thank Dr Alan Kennedy, Department of Pure and Applied Chemistry, for his assistance in modelling the disorder in the single crystal X-ray diffraction and Prof Alastair Florence for access to the Glasgow Physical Organic Chemistry centre facilities.

References

1 N. J. Wheate, S. Walker, G. E. Craig and R. Oun, *Dalton Trans.*, 2010, **39**, 8113–8127.
2 L. Kelland, *Nat. Rev. Cancer*, 2007, **7**, 573–584.
3 D. R. Boer, A. Canals and M. Coll, *Dalton Trans.*, 2009, 399–414.
4 J. Reedijk, *Proc. Natl. Acad. Sci. U. S. A.*, 2003, **100**, 3611–3616.
5 V. Cepeda, M. A. Fuertes, J. Castilla, A. Carlos, C. Quevedo and J. M. Perez, *Anti-Cancer Agents Med. Chem.*, 2007, **7**, 3–18.
6 R. C. Todd and S. J. Lippard, *Metallomics*, 2009, **1**, 280–291.
7 K. Barabas, R. Milner, D. Lurie and C. Adin, *Vet. Comp. Oncol.*, 2008, **6**, 1–18.
8 C. R. Centerwall, D. J. Kerwood, J. Goodisman, B. B. Toms and J. C. Dabrowiak, *J. Inorg. Biochem.*, 2008, **102**, 1044–1049.
9 G. L. Beretta, V. Benedetti, G. Cossa, Y. G. A. Assaraf, E. Bram, L. Gatti, E. Corna, N. Carenini, D. Colangelo, S. B. Howell, F. Zunino and P. Perego, *Biochem. Pharmacol.*, 2010, **79**, 1108–1117.
10 J. B. Mangrum and N. P. Farrell, *Chem. Commun.*, 2010, **46**, 6640–6650.
11 F. Arnesano and G. Natile, *Coord. Chem. Rev.*, 2009, **253**, 2070–2081.
12 M. Hay, *Curr. Opin. Oncol., Endocr. Metab. Invest. Drugs*, 1999, **1**, 443–447.
13 J. Treat, J. Schiller, E. Quoix, A. Mauer, M. Edelman, M. Modiano, P. Bonomi, R. Ramlau and E. Lemarie, *Eur. J. Cancer*, 2002, **38**, S13–S18.
14 Y. Chen, Z. Guo, S. Parsons and P. J. Sadler, *Chem.–Eur. J.*, 1998, **4**, 672–676.
15 J. Holford, F. Raynaud, B. A. Murrer, K. Grimaldi, J. A. Hartley, M. Abrams and L. R. Kelland, *Anti-Cancer Drug Des.*, 1998, **13**, 1–18.
16 V. P. Munk, C. I. Diakos, L. T. Ellis, R. R. Fenton, B. A. Messerle and T. W. Hambley, *Inorg. Chem.*, 2003, **42**, 3582–3590.
17 N. J. Wheate and J. G. Collins, *Coord. Chem. Rev.*, 2003, **241**, 133–145.
18 N. J. Wheate and J. G. Collins, *Curr. Med. Chem.: Anti-Cancer Agents*, 2005, **5**, 267–279.
19 A. Hegmans, S. J. Berners-Price, M. S. Davies, D. S. Thomas, A. S. Humphreys and N. Farrell, *J. Am. Chem. Soc.*, 2004, **126**, 2166–2180.
20 M. B. G. Kloster, J. C. Hannis, D. C. Muddiman and N. Farrell, *Biochemistry*, 1999, **38**, 14731–14737.
21 D. I. Jodrell, T. R. J. Evans, W. Steward, D. Cameron, J. Prendiville, C. Aschele, C. Noberasco, M. Lind, J. Carmichael, N. Dobbs, G. Camboni, B. Gatti and F. De Braud, *Eur. J. Cancer*, 2004, **40**, 1872–1877.
22 T. A. Hensing, N. H. Hanna, H. H. Gillenwater, M. G. Camboni, C. Allievi and M. A. Socinski, *Anti-Cancer Drugs*, 2006, **17**, 697–704.
23 M. E. Oehlsen, Y. Qu and N. Farrell, *Inorg. Chem.*, 2003, **42**, 5498–5506.
24 N. Summa, J. Maigut, R. Puchta and R. van Eldik, *Inorg. Chem.*, 2007, **46**, 2094–2104.
25 M. Sarkar and K. Biradha, *Cryst. Growth Des.*, 2006, **6**, 202–208.
26 R. A. Ruhayel, J. J. Moniodis, X. Yang, J. Kasparkova, V. Brabec, S. J. Berners-Price and N. P. Farrell, *Chem.–Eur. J.*, 2009, **15**, 9365–9374.
27 Y. Qu, M.-C. Tran and N. P. Farrell, *J. Biol. Inorg. Chem.*, 2009, **14**, 969–977.
28 S. Komeda, T. Moulaei, K. K. Woods, M. Chikuma, N. P. Farrell and L. D. Williams, *J. Am. Chem. Soc.*, 2006, **128**, 16092–16103.
29 N. J. Wheate, C. Cullinane, L. K. Webster and J. G. Collins, *Anti-Cancer Drug Des.*, 2001, **16**, 91–98.
30 B. M. Still, P. G. Anil Kumar, J. R. Aldrich-Wright and W. S. Price, *Chem. Soc. Rev.*, 2007, **36**, 665–686.
31 J. Reedijk, *Chem. Rev.*, 1999, **99**, 2499–2510.
32 E. I. Montero, B. T. Benedetti, J. B. Mangrum, M. J. Oehlsen, Y. Qu and N. P. Farrell, *Dalton Trans.*, 2007, 4938–4942.
33 B. P. Esposito and R. Najjar, *Coord. Chem. Rev.*, 2002, **232**, 137–149.
34 C. Møller, H. S. Tastesen, B. Gammelgaard, I. H. Lambert and S. Stürup, *Metallomics*, 2010, **2**, 811–818.
35 L. Trynda-Lemiesz, H. Kozlowski and B. K. Keppler, *J. Inorg. Biochem.*, 1999, **77**, 141–146.
36 A. R. Timerbaev, C. G. Hartinger, S. S. Aleksenko and B. K. Keppler, *Chem. Rev.*, 2006, **106**, 2224–2248.
37 F. Raynaud, F. Boxall, P. Goddard, M. Valenti, M. Jones, B. Murrer, M. Abrams and L. Kelland, *Clin. Cancer Res.*, 1997, **3**, 2063–2074.
38 Y. Qu, H. Rauter, A. P. S. Fontes, R. Bandarage, L. R. Kelland and N. Farrell, *J. Med. Chem.*, 2000, **43**, 3189–3192.
39 J. D. Roberts, G. Beggiolin, C. Manzotti, L. Piazzoni and N. Farrell, *J. Inorg. Biochem.*, 1999, **77**, 47–50.
40 J. D. Roberts, J. Peroutka and N. Farrell, *J. Inorg. Biochem.*, 1999, **77**, 51–57.
41 O. McNoleg, *Comput. Geosci.*, 1996, **22**, 585–588.
42 G. M. Sheldrick, *Acta Crystallogr., Sect. A: Fundam. Crystallogr.*, 2008, **A64**, 112–122.
43 L. J. Farrugia, *J. Appl. Crystallogr.*, 1999, **32**, 837–838.
44 G. M. Sheldrick, *SADABS (Version 2.03)*, 2002.
45 W. I. F. David, K. Shankland, J. van de Streek, E. Pidcock, W. D. S. Motherwell and J. C. Cole, *J. Appl. Crystallogr.*, 2006, **39**, 910–915.
46 G. J. Kirkpatrick, J. A. Plumb, O. B. Sutcliffe, D. J. Flint and N. J. Wheate, *J. Inorg. Biochem.*, 2011, **105**, 1115–1122.
47 S. Sharp, C. O'Neill, P. Rogers, F. Boxall and L. Kelland, *Eur. J. Cancer*, 2002, **38**, 2309–2315.